HemaSphere 🧠 eha

Secondary lesions and sensitivity to signaling inhibitors in iAMP21 acute lymphoblastic leukemia

Femke M. Hormann[1,2,3,^] 🆔 | Anna Østergaard[1,^] 🆔 | Stijn van den Broek[1,2] |
Aurélie Boeree[1,2] | Cesca van de Ven[1,2] 🆔 | Gabriele Escherich[4,5] |
Edwin Sonneveld[1] 🆔 | Judith M. Boer[1,2] 🆔 | Monique L. den Boer[1,2,3] 🆔

Graphical Abstract

Secondary lesions and sensitivity to signaling inhibitors of iAMP21 ALL
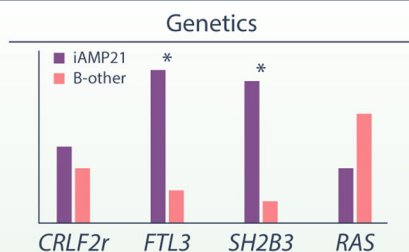
Secondary lesions and sensitivity to signaling inhibitors in iAMP21 acute lymphoblastic leukemia

Femke M. Hormann[1,2,3,^] 🔘 | Anna Østergaard[1,^] 🔘 | Stijn van den Broek[1,2] |
Aurélie Boeree[1,2] | Cesca van de Ven[1,2] 🔘 | Gabriele Escherich[4,5] |
Edwin Sonneveld[1] 🔘 | Judith M. Boer[1,2] 🔘 | Monique L. den Boer[1,2,3] 🔘

Correspondence: Monique L. den Boer (m.l.denboer@prinsesmaximacentrum.nl)

Abstract

Intrachromosomal amplification of chromosome 21 (iAMP21) B-cell precursor acute lymphoblastic leukemia (BCP-ALL) in children is a high-risk subtype for which targeted drugs are lacking. In this study, we determined the frequency of secondary lesions in 28 iAMP21 BCP-ALL patient samples and investigated cellular sensitivity for candidate-targeted drugs. iAMP21 was enriched in *FLT3* aberrations (10.7% vs. 50.0%, $p = 0.003$) and *SH2B3* inactivation (7.14% vs. 46.4%, $p = 0.002$), compared with 28 B-other cases, and these alterations co-occurred in 21.4%. The occurrence of lesions in *CRLF2* and *IL7R* was similar between iAMP21 and B-other cases (25% vs. 17.9%, $p = 0.746$ and 7.14% vs. 0%, $p = 0.491$ respectively) as were mutations in *JAK1* and *JAK2* (3.57% vs. 0% and 10.7% vs. 10.7%, $p = 1$ for both). Sensitivity to the FLT3 inhibitor gilteritinib did not differ between iAMP21 and B-other cases irrespective of FLT3 status. However, iAMP21 samples harboring both *FLT3*-ITD and *SH2B3* lesions showed the highest sensitivity. *CRLF2*-rearranged iAMP21 samples were slightly more sensitive to JAK inhibitor ruxolitinib than those without, although a lack of sensitivity was present in 50% of iAMP21 cases. Trametinib sensitivity varied among iAMP21 samples with over half of iAMP21 samples being sensitive irrespective of RAS-pathway mutation status or other secondary lesions. In summary, iAMP21 leukemias were enriched in *FLT3* and in *SH2B3* lesions, which when co-occurring affected sensitivity to FLT3 inhibition by gilteritinib but not JAK inhibition by ruxolitinib. Together, our results suggest that FLT3 and RAS signaling inhibitors are of interest for further (pre)clinical evaluation in iAMP21 BCP-ALL.

INTRODUCTION

Pediatric B-cell acute lymphoblastic leukemia (BCP-ALL) is the most common childhood malignancy and is characterized by different chromosomal rearrangements. One of these rearrangements is intrachromosomal amplification of chromosome 21 (iAMP21), comprising ~2% of pediatric BCP-ALL.[1,2] iAMP21 BCP-ALL is associated with a poor prognosis when patients are treated on a standard protocol,[1,3] but the prognosis has increased with more intensive treatment.[2,4] However, targeted therapy is needed to reduce toxicity and improve long-term clinical outcomes. Thus far, downstream target genes affected by the iAMP21 have not been identified, and the iAMP21 rearrangement itself cannot be targeted directly.

An iAMP21 is characterized by one abnormal chromosome 21, comprising heterogeneous regions of rearrangements, gains, amplifications, inversions, and losses, arising through a breakage-fusion-bridge mechanism that occurs over several cell cycles.[5–8] BCP-ALL with other structural aberrations of chromosome 21 (osa21) has copy number changes other than the typical pattern of amplifications and losses in the same region of chromosome 21 as iAMP21. These abnormalities have been hypothesized to have the same biological effect.[7] Therefore, we analyzed the osa21 cases together with the iAMP21 cases.

Previous research into secondary lesions showed that lesions in genes affecting the JAK/STAT pathway, such as *SH2B3*,[9–11] *FLT3* (internal tandem duplication [ITD] in particular), *CRLF2*, *IL7R*, *JAK1*, and *JAK2*,[12–15] and lesions affecting the RAS pathway[11,16] are

[1]Princess Máxima Center for Pediatric Oncology, Utrecht, Netherlands
[2]Oncode Institute, Utrecht, Netherlands
[3]Department of Pediatric Oncology and Hematology, Erasmus MC-Sophia Children's Hospital, Rotterdam, Netherlands

[4]COALL–German Cooperative Study Group for Childhood Acute Lymphoblastic Leukemia, Hamburg, Germany
[5]Clinic of Pediatric Hematology and Oncology, University Medical Center Hamburg-Eppendorf, Hamburg, Germany
[^]Femke M. Hormann and Anna Østergaard shared first author.

common in iAMP21 BCP-ALL. Since novel therapies can target several of these lesions, we determined the prevalence of secondary lesions in iAMP21 BCP-ALL and investigated drug sensitivity to targeted inhibitors.

METHODS

Patient samples

Peripheral blood and/or bone marrow samples were obtained from children with newly diagnosed or relapsed BCP-ALL. In accordance with the Declaration of Helsinki, written informed consent to use excess diagnostic material for research purposes was obtained from parents or guardians, as approved by the Medical Ethics Committee of the Erasmus Medical Center, The Netherlands. This study comprised children treated in Dutch Childhood Oncology Group trials (ALL-8, ALL-9, ALL-10, and ALL-11) and two German Cooperative ALL trials (COALL 06-97 and 07-03). Cytogenetic subtype and ploidy status were determined using karyotyping, fluorescence in situ hybridization (FISH), and RT-PCR by reference laboratories. Control patients were selected based on the absence of *BCR::ABL1*, *ABL*-class fusions, *ETV6::RUNX1*, high hyperdiploidy (HeH), low hypodiploidy, near haploid, *KMT2A* rearrangements, *TCF3::PBX1*, as well as somatic or constitutional trisomy 21 (Supporting Information S1: Table S1). iAMP21 patients were selected based on FISH and/or array comparative genomic hybridization (aCGH) data. Mononuclear cells were collected with density gradient centrifugation using Lymphoprep 1.077 g/mL, Nycomed Pharma, Oslo, Norway. Leukemic blast percentage was determined using May-Grünwald-Giemsa staining and if needed, enriched to above 80% using negative bead enrichment.

Patient-derived xenografts (PDX)

Liquid nitrogen cryopreserved viable frozen BCP-ALL cells were thawed for intrafemoral injection into 7- to 12-week-old female NOD.Cg-*Prkdc*^scid *Il2rg*^tm1Wjl/SzJ (NSG) mice (Charles River), as approved by the Central Committee for Animal Experiments of the Dutch Cancer Institute and the Erasmus Medical Center. Per patient sample, three mice were injected with 1 million viable cells each. Leukemic burden was tested every 2–4 weeks by flow cytometry of peripheral blood obtained from the tail. After red blood cell lysis of whole blood, cells were stained with anti-human CD19-BV421, anti-mouse CD45-FITC, and anti-human CD45-PE (all from Biolegend), and leukemic blast percentage was determined. Detectable engraftment was defined as ≥0.5% human CD19-positive cells in peripheral blood. Mice were sacrificed upon overt leukemia, 12 months after injection, or for humane reasons. Leukemic cells were harvested from mouse bone marrow and spleen. The blast percentage of material was confirmed to be above 80% by May-Grünwald-Giemsa staining and flow cytometry using the aforementioned markers. All ex vivo experiments with PDX material were performed in culturing medium, consisting of RPMI Dutch modification, supplemented with 20% fetal calf serum, penicillin, streptomycin, fungizone, gentamicin, L-glutamine, and insuline-transferrin-sodium selenite.

Detecting secondary lesions

Secondary lesions in primary patient samples were determined by aCGH using the Agilent G3 Human 4x180K aCGH array as previously described;[17] multiplex ligation-dependent probe amplification (MLPA) was performed with the SALSA MLPA P335 ALL-*IKZF1* and/or SALSA

MLPA P202 *IKZF1* kit (MRC-Holland), as previously described,[18] and RNA sequencing and whole exome sequencing (WES) is described in more detail in the Supporting Information Methods. All evaluated amino-acid positions and mutations detected by RNA sequencing and WES on these positions are presented in Supporting Information S1: Table S2.

Relevant lesions found in the primary material were validated in PDX material by genomic PCR, reverse transcriptase PCR, and WES and analyzed for new lesions in *FLT3*, *SH2B3*, *CRLF2*, and *JAK1/2* as described in more detail in the Supporting Information Methods and Supporting Information S1: Table S3.

Drug exposure tests

Activation of signaling pathways and drug sensitivity was measured in the generated PDX material and primary material if possible. A detailed description is given in the Supporting Information Methods. If multiple primary or PDX samples of the same patient were present and the material presented the same secondary lesions, results were combined and analyzed together. This led to data on 12 different iAMP21 and 3 B-other cases (Supporting Information S1: Figure S1).

Statistics

Nominal values were tested with a Fisher exact test. Numerical variables were compared between groups with the Wilcoxon Rank Sum test. Data were considered significant if the $p < 0.05$. For expression data, false discovery rate correction was performed according to the Benjamini-Hochberg method by the EdgeR_3.32.1 package in R version 4.0.2.

RESULTS

Patient cohort

To identify secondary lesions in iAMP21 BCP-ALL, we performed total RNA sequencing on diagnostic samples from 25 iAMP21, 3 osa21, and 28 B-other patients without a chromosome 21 aberration based on aCGH and/or karyotype (Supporting Information S1: Table S1).

Frequency of lesions in the JAK/STAT pathway

We evaluated lesions in 23 common leukemia-associated genes and found 20 genes altered in at least two samples in the total cohort of 56 patients (Figure 1 and Supporting Information S1: Tables S4–S6). iAMP21 BCP-ALL was enriched in secondary lesions in the JAK/STAT pathway compared with B-other (82.1% vs. 35.7%, $p < 0.001$), including internal tandem duplications (ITD) ($n = 6$), other activating lesions ($n = 3$), and overexpression ($n = 5$) of the cytokine receptor gene *FLT3* (50.0% vs. 10.7%, $p = 0.003$, Figures 1 and 2A and Supporting Information S1: Figure S2). In contrast, the frequencies of lesions in genes encoding cytokine receptors *CRLF2* and *IL7R* were similar between iAMP21 and B-other cases (25% vs. 17.9%, $p = 0.746$ and 7.14% vs. 0%, $p = 0.491$, respectively) as were mutations in *JAK1* and *JAK2* (3.57% vs. 0% and 10.7% vs. 10.7% respectively, $p = 1$ for both).

Of the 28 iAMP21/osa21 samples, six showed homozygous *SH2B3* mutations and four homozygous deletions of the gene (Supporting Information S1: Figures S3 and S4). These cases showed a lack of *SH2B3* expression in RNA sequencing data, as did 3 other cases without apparent lesions in *SH2B3*. Together, 13 *SH2B3*
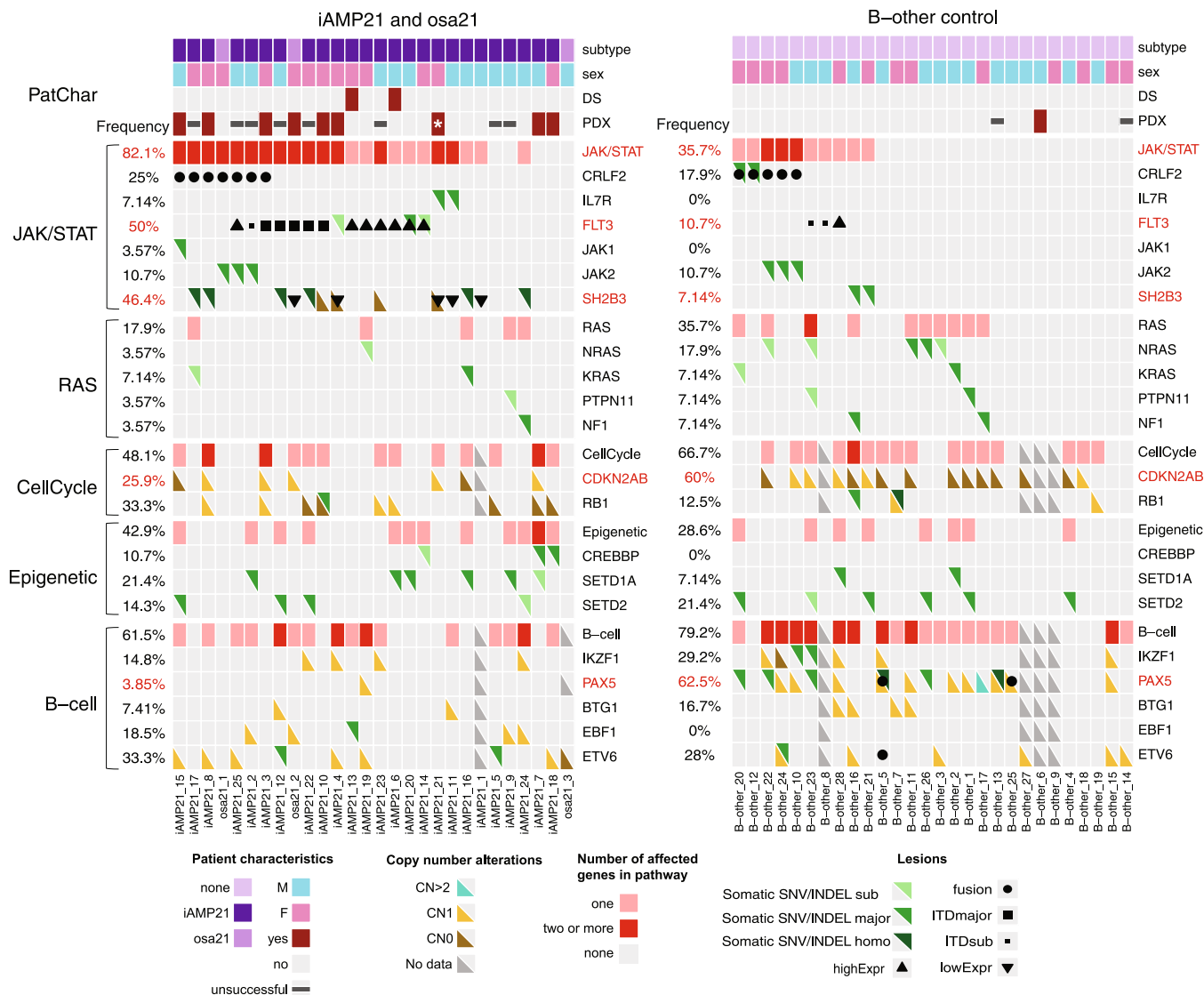
FIGURE 1 Oncoprint of patient characteristics and identified mutations in iAMP21/osa21 and B-other samples. Within the 28 B-other samples, there were 4 *DUX4*-rearranged, 1 *EPOR* fusion, 2 *MEF2D*-rearranged, and 1 *NUTM1*-rearranged. Variants and gene fusions were identified with total RNA sequencing, with a minimal VRF of 10%. Copy number alterations of *CDKN2A/B, RB1, IKZF1, PAX5, BTG1, EBF1,* and *ETV6* were determined with MLPA.[18] Refer to Supporting Information S1: Table S4 for the specific mutations. Low expression cutoff is based on a z-score below −2 for *SH2B3*. High expression is defined by expression >1000 fragments per kilobase per million for *FLT3*. Frequencies with statistically significant *p*-values are shown in red. More detailed statistics are displayed in Supporting Information S1: Table S6. CN > 2 refers to a copy number gain, CN1 to a deletion, and CN0 to a homozygous deletion. Minor clone SNV/indel VRF < 25%, Major clone 25% ≤ VRF < 75%, homozygous VRF ≥ 75%, Minor clone FLT3-ITD VRF < 50%, Major clone ≥50%. *indicates PDX engrafted with <30% blasts in the spleen.

aberrations were detected in iAMP21 cases (46.4%). In contrast, two B-other cases with heterozygous *SH2B3* mutations had an expression of *SH2B3* (Figure 1). Together these data suggest that the inactivation of *SH2B3*, the downstream negative regulator of JAK/STAT and FLT3 signaling, is more frequent in iAMP21 cases than in B-other cases (46.4% vs. 7.14%, *p* = 0.002). *SH2B3* lesions co-occurred with *FLT3* lesions, *CRLF2* rearrangements, and *IL7R* mutations, while *JAK1* or *JAK2* mutations co-occurred with *CRLF2* rearrangement in *SH2B3* wildtype iAMP21 and B-other cases. These data suggest that cytokine receptor aberrations synergize with lesions in downstream signaling regulators to activate the JAK/STAT pathway in iAMP21 BCP-ALL. The frequency of lesions in RAS pathway genes did not differ between iAMP21 and B-other cases (17.9% vs. 35.7%, *p* = 0.227, Figure 1).

Frequency of lesions in cell cycle and B-cell development genes

Overall, lesions in cell cycle genes had a similar frequency between iAMP21 and B-other cases (48.1% vs. 66.7%, *p* = 0.26). However, in B-other cases, most of the lesions were found in *CDKN2A/B* while in iAMP21 cases the lesions were skewed toward *RB1* (Figure 1). All lesions in both iAMP21 and B-other cases in epigenetic genes were mutations and these were distributed similarly between the two groups.

Overall, lesions in B-cell development genes including *IKZF1* and *EBF1* were as frequent in iAMP21 as in B-other cases. *PAX5* deletions, however, were less frequent in iAMP21 cases compared with B-other (3.85% vs. 62.5%, *p* < 0.001, Figure 1). Interestingly, *PAX5*
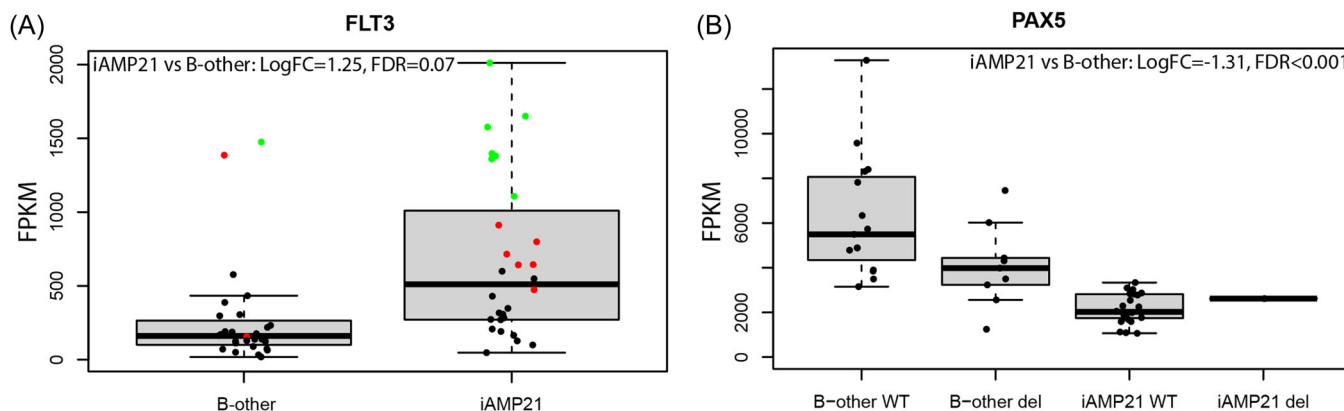
FIGURE 2 Evaluation of differential gene expression in iAMP21/osa21. **(A)** *FLT3* expression in FPKM in iAMP21/osa21 and B-other. *FLT3*-ITD samples are indicated in red, and samples with a high wildtype *FLT3* expression (FPKM > 1000) are indicated in green. **(B)** *PAX5* expression in FPKM in iAMP21/osa21 and B-other, divided by *PAX5* wildtype and *PAX5* deleted as shown in Figure 1. Samples with unknown *PAX5* copy number status were excluded. **(A, B)** Boxplots indicate median and interquartile range, with whiskers extending to the furthest dot, at a maximum of 1.5 times the interquartile range. del, deleted; FDR, false discovery rate adjusted *p*-value; FPKM, fragments per kilobase per million mapped fragments; LogFC, log-fold change; WT, wildtype.

gene expression was significantly decreased in iAMP21 compared with B-other, both for *PAX5* wildtype and deleted cases (iAMP21 vs. B-other log2 fold change = −1.31, *p* < 0.001, Figure 2B). *PAX5* is part of a transcriptional network, including *IKZF1*, *EBF1*, *SPI1*, and *IRF4*,[19] and reduced expression co-occurred with reduced *SPI1* and *IRF4* expression in these iAMP21 samples (Supporting Information S1: Figure S5). Together these data suggest that iAMP21 BCP-ALL has a distinct landscape of cell cycle and B-cell development gene aberrations that affect transcription and thereby cell signaling pathways.

Establishment of iAMP21 xenografts

To obtain material for studying the effect of the secondary lesions on sensitivity to targeted drugs, we generated PDX from 17 available iAMP21 ALL and three randomly selected B-other patients. Engraftment success and time were variables within the same patient material and between material from different patients (Figure 3A and Supporting Information S1: Figure S6). Eventually, eight iAMP21 and one B-other sample successfully engrafted in at least one of three injected mice within 14 months (Figure 3A). In iAMP21 samples, engraftment success was affected by the number of lesions in cell cycle genes with samples harboring two lesions having the highest engraftment success rate with 7 out of 9 samples engrafting (0 vs. 1 vs. 2 lesions *p* = 0.02; Figure 1). The median time to detectable engraftment was 6.3 months, ranging from 2 to 11 months, and the median time to harvest was 8.9 months, ranging from 2.1 to 15.5 months, and did not depend on secondary lesions present. The number of leukemic cells harvested from the spleen highly varied from less than 100 million to 1.6 billion and did not correlate with the peripheral blood blast percentage taken at the harvesting timepoint (Supporting Information S1: Figure S6). Secondary lesions were determined in the PDX material, and an overview is presented in the Supporting Information S1: Figure S1. *FLT3*-ITD was conserved in 3/3 PDX samples from one patient (iAMP21-3), 1/2 PDX sample from another patient (iAMP21-10), while it was lost in 2/2 PDX samples from a third patient (osa21-2; Figure 3B, Supporting Information S1: S7A and S7D). *SH2B3* deletion was conserved in all PDX samples of four patients (osa21-2 and iAMP21-4, iAMP21-8, iAMP21-10) (Figure 3B and Supporting Information S1: Figure S7B,S7C). The *P2RY8::CRLF2* fusion was retained in all samples from three patients (iAMP21-3, iAMP21-8, iAMP21-15; Figure 3B and Supporting Information S1:

Figure S7E). The *JAK1* mutation was retained in 3/3 PDX samples (iAMP21-15; Figure 3B and Supporting Information S1: Figure S7F). In total, 18 iAMP21 PDX samples, originating from eight primary samples, were used in ex vivo studies with targeted inhibitors (Figure 3B and Supporting Information S1: Figure S1).

Response to pathway activation

The JAK/STAT pathway is mainly regulated by the IL7R, CRLF2, and FLT3 receptors, which respond to IL7, TSLP, and FLT3-ligand (FLT3L) respectively, and via downstream regulators JAK1/2/3, SH2B3, and RAS lead to intracellular STAT5, AKT, and ERK phosphorylation (Figure 4). Due to the high number of genetic lesions affecting JAK/STAT pathway genes in the iAMP21 cases, we studied the effect of pathway stimulation with these three ligands.

After 4 days of exposure to the ligands metabolic activity was increased, without increasing the number of cells (Supporting Information S1: Figure S8). We then assessed the baseline and stimulated phosphorylation levels of STAT5, AKT, and ERK in nine samples from seven patients. None of the samples showed protein phosphorylation without ligand stimulation, including the sample harboring an *FLT3*-ITD where ligand-independent activation would be expected (Supporting Information S1: Figure S9). IL7 and TSLP led to higher phosphorylation levels of AKT, ERK, and STAT5 than FLT3L (Supporting Information S1: Figure S9). This was observed in samples with *SH2B3* aberration (four patients), with *FLT3*-ITD and *CRLF2* rearrangement (1 patient), and without JAK/STAT pathway aberrations (two patients). This limited representation of genetic aberrations did not show associations between ligand stimulation and AKT/STAT5/ERK phosphorylation. With triple stimulation, using a cocktail of the three ligands, all samples showed similar phosphorylation levels of AKT/STAT5/ERK. Since the three ligands are expected to be present in the leukemic microenvironment, further drug sensitivity experiments were performed in the presence of a three-ligand cocktail containing IL7, TSLP, and FLT3L.

Ex vivo drug sensitivity

First, we tested the sensitivity of iAMP21 BCP-ALL to four commonly used induction drugs (prednisolone, vincristine, daunorubicin, and
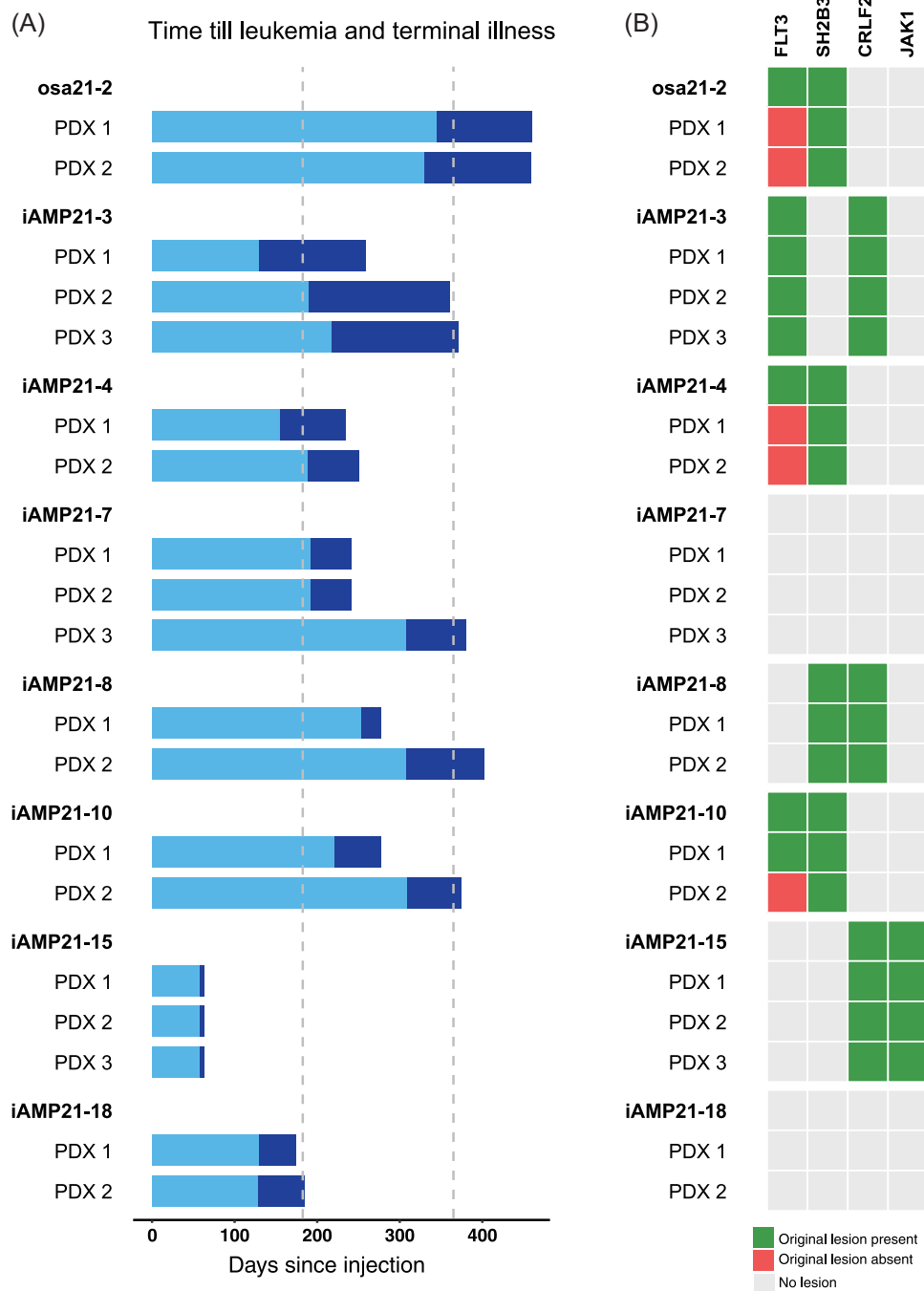
FIGURE 3 Engraftment of PDX samples. (A) Overview of samples that were used for engraftment in PDX. Length of the bar indicates the time till the sacrifice of the mouse. Light blue bar indicates the time till leukemic cells were measurable in peripheral blood, and dark blue indicates the time the mouse was positive for leukemic engraftment until harvest. Time is indicated in days from the day of injection, with a dotted line at a half year and 1 year. All samples had a leukemic content of at least 80% blasts in the spleen upon harvest. (B) Summary of validation of secondary lesions in PDX. Shown more elaborately in Supporting Information S1: Figure S7A–F. Green indicates that the lesion was retained in the PDX material, while red indicates the lesion was absent in the PDX material.

asparaginase). iAMP21 showed similar sensitivity to these drugs as previously described B-other BCP-ALL[20] (Supporting Information S1: Figure S10). To determine whether the iAMP21 subtype might benefit from targeted inhibitors gilteritinib (FLT3), trametinib (MEK), or ruxolitinib (JAK1/2), we exposed primary and PDX material to these drugs. If multiple samples of the same patient harboring the same secondary lesions were tested, they were analyzed together.

All individual drug sensitivity curves are presented in Supporting Information S1: Figures S11–13. The grouping of samples based on secondary lesions is described in Supporting Information S1: Figure S1.

Gilteritinib sensitivity did not differ between iAMP21 and B-other cases (median LC50 1.24 µM, range 0.33–4.85 µM vs. median LC50 1.21 µM, range 1.20–1.3 µM, $p = 0.95$). Samples with both
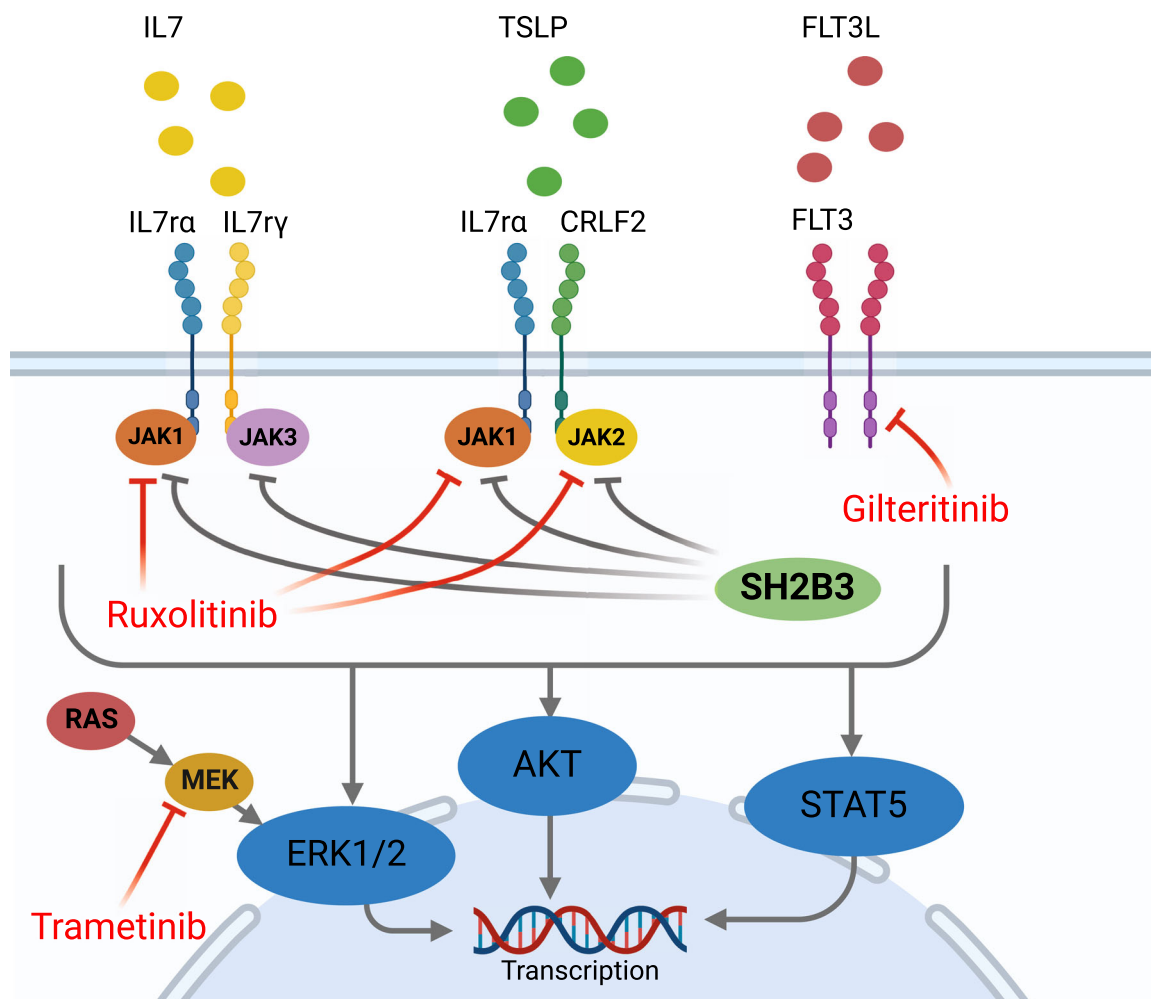
FIGURE 4 Pathways of drugs evaluated in iAMP21, osa21, and B-other BCP-ALL samples.

FLT3-ITD and *SH2B3* lesions had the highest sensitivity to gilteritinib (median LC50 0.39 μM, range 0.35–0.43 μM, Figure 5A,B, *p* > 0.2). Samples with only *FLT3* or *SH2B3* lesions did not show increased sensitivity compared with those without these lesions (*p* > 0.5 for both, Figure 5A,B). Interestingly, the relapse sample of iAMP21-12 that lost *FLT3*-ITD also became less sensitive to gilteritinib when compared with the sample taken at diagnosis, although not significant (Supporting Information S1: Figure S11).

Median ruxolitinib sensitivity did not significantly differ between iAMP21 and B-other samples (median LC50 8.38 μM, range 1.00 to >10 μM, vs. median LC50 0.48, range 0.21 to >10 μM; *p* = 1). Extreme resistance to ruxolitinib seemed more frequent in iAMP21 samples (6 out of 12 iAMP21 cases had LC50 > 10 μM) but this was not related to *FLT3* or *SH2B3* status (Figure 4C,D). *CRLF2*r iAMP21 cases were slightly more sensitive to ruxolitinib than those lacking *CRLF2* rearrangement, although this difference did not reach significance (median LC50 4.72 μM, range 1.0–4.85 vs. median LC50 > 10 μM, range 2.66 to >10 μM; *p* = 0.08). The highest sensitivity for ruxolitinib in iAMP21 was found in iAMP21-15 with both a *CRLF2* rearrangement and a *JAK1* mutation (LC50 of 1.00 μM, Figure 5C,D). iAMP21-15 also increased the most in metabolic activity upon TSLP stimulation (Supporting Information S1: Figure S8B).

A large variation was present in trametinib sensitivity among both iAMP21 and B-other samples (median LC50 0.11 μM, range 0.017 to >5 μM vs. median LC50 0.18, range 0.018 to >5 μM; *p* = 0.72, Figure 5E,F). More than half of iAMP21 cases were sensitive irrespective of RAS pathway lesion status (Figure 5E,F). Of these sensitive samples, one had a subclonal *KRAS* mutation, and none of the other samples showed mutations in *KRAS*, *NRAS*, *PTPN11*, or *NF1*.

DISCUSSION

In this study, we showed that JAK/STAT pathway lesions, in particular those affecting *SH2B3* and *FLT3*, were more frequent in iAMP21 cases while the frequency of RAS pathway lesions was similar to B-other cases. *FLT3*-ITD in combination with *SH2B3* lesions resulted in the highest gilteritinib sensitivity and *CRLF2* fusions resulted in increased ruxolitinib sensitivity, although not statistically significant. Surprisingly, about half of iAMP21 cases were sensitive to trametinib, irrespective of RAS pathway mutation status.

Similar to other studies reporting on iAMP21 xenografts,[9,21,22] our xenografts engrafted at a slow rate,[23] and successful xenografts were enriched in cell cycle gene lesions.[21,24] Clonal heterogeneity during engraftment can affect the presence of secondary lesions in the PDX material as previously described by Sinclair et al. in iAMP21 ALL[21] and described by our group in *JAK*-mutated ALL.[25] Since murine TSLP does not bind to human TSLPR,[26] one could expect a loss of *CRLF2*
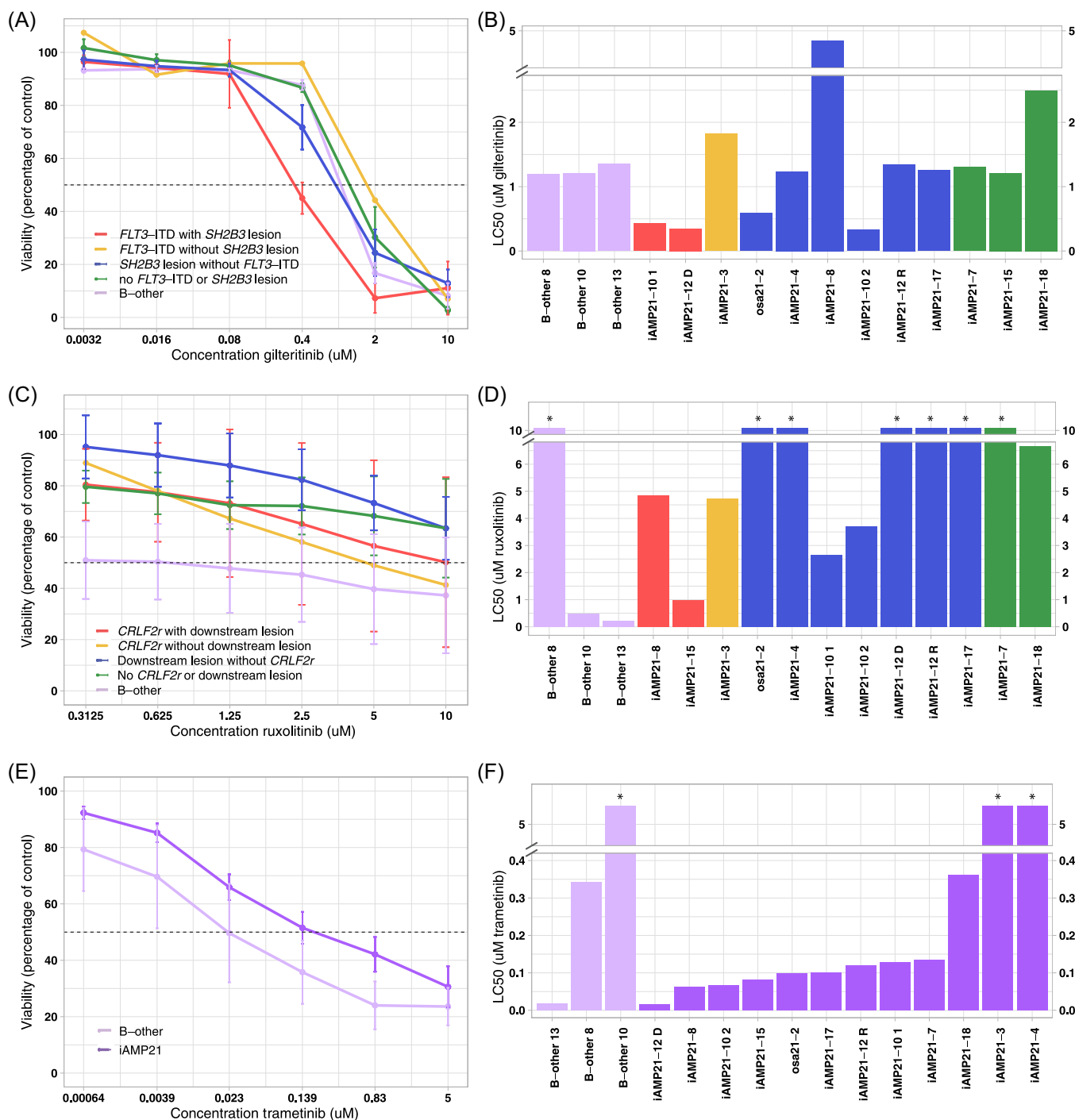
FIGURE 5 Sensitivity to the targeted drugs—gilteritinib, ruxolitinib, and trametinib in iAMP21 ALL. Dose-response curves display the mean and standard error of the mean. If multiple samples were present in one case, LC50 is summarized by the mean of all samples per case. Refer to Supporting Information S1: Figure S1 for included cases per graph and per group. All individual curves can be found in Supporting Information S1: Figures S11–S13. (A) Dose-response curve to gilteritinib of B-other and iAMP21 cases grouped by *FLT3*-ITD and secondary lesion. (B) Sensitivity to gilteritinib of individual cases grouped by *FLT3*-ITD and secondary lesion. (C) Dose-response curve to ruxolitinib of B-other and iAMP21 cases grouped by *CRLF2* rearrangement and secondary lesion. (D) Sensitivity to ruxolitinib of individual B-other and iAMP21 cases grouped by *CRLF2* rearrangement and secondary lesion. (E) Dose-response curve to trametinib of B-other and iAMP21 cases. (F) Sensitivity to trametinib of individual B-other and iAMP21 cases. *indicates that LC50 was not reached within the drug dose range.

rearrangements due to a lack of survival benefit in mice. We did, however, only observe a loss of *FLT3*-ITD in PDX material even though murine FLT3L also binds the human FLT3 receptor.[27] This underlines the importance of validation of secondary lesions after expansion in PDX before

evaluating the efficacy of targeted drugs.[28] Patterns of cytokine receptor lesion loss can also occur in the evolution from initial diagnosis to relapse in patients as previously shown for *FLT3*-ITD and *CRLF2* rearrangement.[29–31] This was also evident in our diagnosis/relapse pair that lost

FLT3-ITD at relapse. In *FLT3*-ITD positive acute myeloid leukemia (AML), the lesion is reported lost at relapse in 46% of patients when treated with targeted drugs.[29] Without targeted therapy ~18% still lose *FLT3*-ITD at relapse, but new ITD or activating mutations can also be acquired in AML and a similar mechanism might be present in ALL[29,30] underlining the importance of reassessing secondary lesions at relapse.[30]

As has been described in other studies,[9–11,32,33] we found that iAMP21 cases were enriched in *FLT3* and *SH2B3* lesions although the frequencies observed in our cohort were higher than previously reported, possibly since we also included *FLT3* overexpression as an activating, and low *SH2B3* expression as inactivating lesion due to their possible effect on gilteritinib sensitivity. This might also contribute to the higher frequency of JAK/STAT pathway lesions: 82.1% in our cohort versus 64% in the cohort of Gao et al. including 124 iAMP21 cases.[11] In contrast, Gao et al. reported more RAS pathway lesions than observed in our cohort: 41% versus 17.9%, respectively, possibly due to the inability to detect *NF1* deletions in our RNA-sequencing-based approach.[11] Frequencies of lesions in cell cycle, B-cell differentiation, and epigenetic genes were similar in both cohorts.

Both our data and Sinclair et al.[34] show that *SH2B3* deletion leads to increased STAT5 phosphorylation[35] in line with others suggesting that *SH2B3* is a negative regulator of the JAK/STAT pathway.[12,13] In our data, *SH2B3* inactivation often co-occurred with cytokine receptor lesions. Therefore, it is likely that *SH2B3* deletions synergize with activating lesions in the cytokine receptor genes (*CRLF2*, *IL7R*, *FLT3*) to disrupt and perhaps bypass normal signaling via these pathways. The highest sensitivity to gilteritinib was present in cases with *FLT3*-ITD and *SH2B3* inactivation, illustrating this possible synergy between cytokine receptors and downstream lesions. In AML, *FLT3*-ITD with an allelic ratio over 50%, is described as a poor prognostic factor[36] and is treated in certain protocols with an FLT3 inhibitor. However, the combined effect of *FLT3*-ITD and *SH2B3* inactivation on prognosis has not been studied so far in either AML or ALL. Based on our data we cannot draw conclusions on its prognostic effect, but our data suggest that FLT3 inhibition might be effective for iAMP21 BCP-ALL with *FLT3*-ITD and *SH2B3* inactivation. Unfortunately, we were limited by the amount of available material to two patients for testing this clinically highly interesting sensitivity to gilteritinib.

In vitro sensitivity at diagnosis to induction drugs has been associated with treatment response.[37–39] Since iAMP21 BCP-ALL is associated with a poor prognosis when patients are treated on a standard protocol,[1,3] we expected more resistance compared with B-other when testing sensitivity to induction drugs. However, we found similar ex vivo sensitivity to prednisolone, asparaginase, vincristine, and daunorubicine. The higher relapse rates despite similar induction drug sensitivity underline the need for novel therapies such as cell signaling inhibitors in iAMP21 BCP-ALL. Of the cell signaling inhibitors we tested, ruxolitinib sensitivity was highest in iAMP21 and B-other samples with both *CRLF2*r and *JAK1* mutation, which is in line with ruxolitinib mainly targeting JAK1/2 while *SH2B3* mainly targets JAK3.[9,12] We also found that downstream lesions might contribute to ruxolitinib sensitivity even without the presence of *CRLF2* rearrangements. The NCT02723994 trial in pediatric de novo high-risk BCP-ALL includes *SH2B3* inactivation, the downstream lesion most present in our cohort, as an inclusion criterion for treatment with ruxolitinib. The results of this trial are expected to elucidate the predictive value of *SH2B3* lesions on clinical ruxolitinib sensitivity.[35]

We found sensitivity to trametinib in more than half of iAMP21 cases, while none had RAS pathway lesions. Trametinib is known to be particularly effective in primary ALL samples with RAS pathway mutations,[40] but its effectiveness has been described in non-mutated samples as well.[40,41] As other pathways, such as *CRLF2*,[14,42] can also signal via MEK-ERK, sensitivity to trametinib is not surprising in RAS pathway wildtype samples. The two iAMP21 cases that were not sensitive to trametinib did, surprisingly, show ERK phosphorylation

upon ligand stimulation. This underlines the complexity of and the need for more research into the specific mechanisms of action of these MEK-ERK inhibitors.

In conclusion, we showed that iAMP21 leukemias are enriched in *FLT3* and *SH2B3* lesions, which when co-occurring, affect sensitivity to FLT3 inhibition by gilteritinib but do not affect JAK inhibition by ruxolitinib. This suggests these lesions act synergistically and might bypass downstream JAK/STAT signaling, which is of interest to further evaluate (pre)clinically in iAMP21 BCP-ALL patients harboring both lesions. Despite the absence of secondary lesions or protein markers linked to sensitivity, leukemic cells from iAMP21 BCP-ALL cases were often sensitive to trametinib. These results suggest that these FLT3 and RAS signaling inhibitors are of interest for further pre-clinical evaluation in iAMP21 BCP-ALL to define suitable markers for selecting patients benefiting from these targeted inhibitors.

AUTHOR CONTRIBUTIONS

The project was conceived by Judith M. Boer and Monique L. den Boer and conceptualized together with Femke M. Hormann. Experimental and computational analyses were performed by Femke M. Hormann, Anna Østergaard, Stijn van den Broek, Aurélie Boeree, and Cesca van de Ven. Clinical samples were provided by Gabriele Escherich and Edwin Sonneveld. Data interpretation was performed by Femke M. Hormann, Anna Østergaard, Judith M. Boer, and Monique L. den Boer. The manuscript was drafted by Femke M. Hormann, Anna Østergaard, Judith M. Boer, and Monique L. den Boer. All authors approved the manuscript.

DATA AVAILABILITY STATEMENT

The data that support the findings of this study are available from the corresponding author upon reasonable request.

ETHICS STATEMENT

In accordance with the Declaration of Helsinki, written informed consent to use excess diagnostic material for research purposes was obtained from parents or guardians, as approved by the Medical Ethics Committee of the Erasmus Medical Center, The Netherlands.

ORCID

Femke M. Hormann https://orcid.org/0000-0001-5164-3047
Anna Østergaard http://orcid.org/0000-0003-2443-421X
Cesca van de Ven http://orcid.org/0000-0002-9797-9539
Edwin Sonneveld https://orcid.org/0000-0002-1869-0957
Judith M. Boer http://orcid.org/0000-0003-4848-7789
Monique L. den Boer https://orcid.org/0000-0002-5795-2921

SUPPORTING INFORMATION

Additional supporting information can be found in the online version of this article.

REFERENCES

1. Heerema NA, Carroll AJ, Devidas M, et al. Intrachromosomal amplification of chromosome 21 is associated with inferior outcomes in children with acute lymphoblastic leukemia treated in contemporary standard-risk children's oncology group studies: a report from the children's oncology group. *J Clin Oncol.* 2013;31:3397-3402.

2. Moorman AV, Robinson H, Schwab C, et al. Risk-directed treatment intensification significantly reduces the risk of relapse among children and adolescents with acute lymphoblastic leukemia and intrachromosomal amplification of chromosome 21: a comparison of the MRC ALL97/99 and UKALL2003 trials. *J Clin Oncol.* 2013;31:3389-3396.

3. Moorman AV, Richards SM, Robinson HM, et al. Prognosis of children with acute lymphoblastic leukemia (ALL) and intrachromosomal amplification of chromosome 21 (iAMP21). *Blood.* 2007;109:2327-2330.

4. Harrison CJ, Moorman AV, Schwab C, et al. An international study of intrachromosomal amplification of chromosome 21 (iAMP21): cytogenetic characterization and outcome. *Leukemia.* 2014;28:1015-1021.

5. Li Y, Schwab C, Ryan SL, et al. Constitutional and somatic rearrangement of chromosome 21 in acute lymphoblastic leukaemia. *Nature.* 2014;508:98-102.

6. Robinson HM, Harrison CJ, Moorman AV, Chudoba I, Strefford JC. Intrachromosomal amplification of chromosome 21 (iAMP21) may arise from a breakage-fusion-bridge cycle. *Genes Chromosom Cancer.* 2007;46:318-326.

7. Rand V, Parker H, Russell LJ, et al. Genomic characterization implicates iAMP21 as a likely primary genetic event in childhood B-cell precursor acute lymphoblastic leukemia. *Blood.* 2011;117:6848-6855.

8. Sinclair PB, Parker H, An Q, et al. Analysis of a breakpoint cluster reveals insight into the mechanism of intrachromosomal amplification in a lymphoid malignancy. *Hum Mol Gen.* 2011;20:2591-2602.

9. Sinclair PB, Ryan S, Bashton M, et al. SH2B3 inactivation through CN-LOH 12q is uniquely associated with B-cell precursor ALL with iAMP21 or other chromosome 21 gain. *Leukemia.* 2019;33:1881-1894.

10. Baughn L, Meredith M, Oseth L, Smolarek T, Hirsch B. SH2B3 aberrations enriched in iAMP21 B lymphoblastic leukemia. *Cancer Genet.* 2018;226-227:30-35.

11. Gao Q, Ryan SL, Iacobucci I, et al. The genomic landscape of acute lymphoblastic leukemia with intrachromosomal amplification of chromosome 21. *Blood.* 2023;142:711-723. doi:10.1182/blood.2022019094

12. Cheng Y, Chikwava K, Wu C, et al. LNK/SH2B3 regulates IL-7 receptor signaling in normal and malignant B-progenitors. *J Clin Invest.* 2016;126:1267-1281.

13. Lin DC, Yin T, Koren-Michowitz M, et al. Adaptor protein Lnk binds to and inhibits normal and leukemic FLT3. *Blood.* 2012;120:3310-3317.

14. Tasian SK, Doral MY, Borowitz MJ, et al. Aberrant STAT5 and PI3K/mTOR pathway signaling occurs in human CRLF2-rearranged B-precursor acute lymphoblastic leukemia. *Blood.* 2012;120:833-842.

15. Choudhary C, Brandts C, Schwable J, et al. Activation mechanisms of STAT5 by oncogenic Flt3-ITD. *Blood.* 2007;110:370-374.

16. Ryan SL, Matheson E, Grossmann V, et al. The role of the RAS pathway in iAMP21-ALL. *Leukemia.* 2016;30:1824-1831.

17. Boer JM, Steeghs EMP, Marchante JRM, et al. Tyrosine kinase fusion genes in pediatric BCR-ABL1-like acute lymphoblastic leukemia. *Oncotarget.* 2017;8:4618-4628.

18. Steeghs EMP, Boer JM, Hoogkamer AQ, et al. Copy number alterations in B-cell development genes, drug resistance, and clinical outcome in pediatric B-cell precursor acute lymphoblastic leukemia. *Sci Rep.* 2019;9:4634.

19. Katerndahl CDS, Heltemes-Harris LM, Willette MJL, et al. Antagonism of B cell enhancer networks by STAT5 drives leukemia and poor patient survival. *Nat Immunol.* 2017;18:694-704.

20. Steeghs EMP, Boer JM, Hoogkamer AQ, et al. Copy number alterations in B-cell development genes, drug resistance, and clinical outcome in pediatric B-cell precursor acute lymphoblastic leukemia. *Sci Rep.* 2019;9:4634.

21. Sinclair PB, Blair HH, Ryan SL, et al. Dynamic clonal progression in xenografts of acute lymphoblastic leukemia with intrachromosomal amplification of chromosome 21. *Haematologica.* 2018;103:634-644.

22. Laurent AP, Siret A, Ignacimouttou C, et al. Constitutive activation of RAS/MAPK pathway cooperates with trisomy 21 and is therapeutically exploitable in down syndrome B-cell leukemia. *Clin Cancer Res.* 2020;26:3307-3318.

23. Frismantas V, Dobay MP, Rinaldi A, et al. Ex vivo drug response profiling detects recurrent sensitivity patterns in drug-resistant acute lymphoblastic leukemia. *Blood.* 2017;129:e26-e37.

24. Clappier E, Gerby B, Sigaux F, et al. Clonal selection in xenografted human T cell acute lymphoblastic leukemia recapitulates gain of malignancy at relapse. *J Exp Med.* 2011;208:653-661.

25. Steeghs EMP, Jerchel IS, de Goffau-Nobel W, et al. JAK2 aberrations in childhood B-cell precursor acute lymphoblastic leukemia. *Oncotarget.* 2017;8:89923-89938.

26. Savino AM, Izraeli S. On mice and humans: the role of thymic stromal lymphopoietin in human B-cell development and leukemia. *Haematologica.* 2016;101:391-393.

27. Ding Y, Wilkinson A, Idris A, et al. FLT3-ligand treatment of humanized mice results in the generation of large numbers of CD141+ and CD1c+ dendritic cells in vivo. *J Immunol.* 2014;192:1982-1989.

28. Frismantas V, Dobay MP, Rinaldi A, et al. Ex vivo drug response profiling detects recurrent sensitivity patterns in drug-resistant acute lymphoblastic leukemia. *Blood.* 2017;129:e26-e37.

29. Schmalbrock LK, Dolnik A, Cocciardi S, et al. Clonal evolution of acute myeloid leukemia with FLT3-ITD mutation under treatment with midostaurin. *Blood.* 2021;137:3093-3104.

30. Kottaridis PD, Gale RE, Langabeer SE, Frew ME, Bowen DT, Linch DC. Studies of FLT3 mutations in paired presentation and relapse samples from patients with acute myeloid leukemia: implications for the role of FLT3 mutations in leukemogenesis, minimal residual disease detection, and possible therapy with FLT3 inhibitors. *Blood.* 2002;100:2393-2398.

31. Vesely C, Frech C, Eckert C, et al. Genomic and transcriptional landscape of P2RY8-CRLF2-positive childhood acute lymphoblastic leukemia. *Leukemia.* 2017;31:1491-1501.

32. Capela de Matos R, Othman M, Ferreira G, et al. Somatic homozygous loss of SH2B3, and a non-Robertsonian translocation t(15;21)(q25.3;q22.1) with NTRK3 rearrangement, in an adolescent with progenitor B-cell acute lymphoblastic leukemia with the iAMP21. *Cancer Genet.* 2022;262-263:16-22.

33. Ivanov Öfverholm I, Tran AN, Olsson L, et al. Detailed gene dose analysis reveals recurrent focal gene deletions in pediatric B-cell precursor acute lymphoblastic leukemia. *Leuk Lymphoma.* 2016;57:2161-2170.

34. Sinclair PB, Ryan S, Bashton M, et al. SH2B3 inactivation through CN-LOH 12q is uniquely associated with B-cell precursor ALL with iAMP21 or other chromosome 21 gain. *Leukemia.* 2019;33:1881-1894.

35. Cheng Y, Chikwava K, Wu C, et al. LNK/SH2B3 regulates IL-7 receptor signaling in normal and malignant B-progenitors. *J Clin Invest.* 2016;126:1267-1281.

36. Cucchi DGJ, Denys B, Kaspers GJL, et al. RNA-based FLT3-ITD allelic ratio is associated with outcome and ex vivo response to FLT3 inhibitors in pediatric AML. *Blood.* 2018;131:2485-2489.

37. Kaspers GJL, Pieters R, Van Zantwijk CH, VanWering ER, Van Der Does-Van Den Berg A, Veerman AJP. Prednisolone resistance in childhood acute lymphoblastic leukemia: vitro-vivo correlations and cross-resistance to other drugs. *Blood.* 1998;92:259-266.

38. Pieters R, Huismans DR, Loonen AH, et al. Relation of cellular drug resistance to long-term clinical outcome in childhood acute lymphoblastic leukaemia. *Lancet.* 1991;338:399-403.

39. Den Boer ML, Harms DO, Pieters R, et al. Patient stratification based on prednisolone-vincristine-asparaginase resistance profiles in children with acute lymphoblastic leukemia. *J Clin Oncol.* 2003;21:3262-3268.

40. Jerchel IS, Hoogkamer AQ, Ariës IM, et al. RAS pathway mutations as a predictive biomarker for treatment adaptation in pediatric B-cell precursor acute lymphoblastic leukemia. *Leukemia*. 2018;32:931-940.

41. Kerstjens M, Driessen EMC, Willekes M, et al. MEK inhibition is a promising therapeutic strategy for MLL-rearranged infant acute lymphoblastic leukemia patients carrying RAS mutations. *Oncotarget*. 2017;8:14835-14846.

42. Meyer LK, Delgado-Martin C, Maude SL, Shannon KM, Teachey DT, Hermiston ML. CRLF2 rearrangement in Ph-like acute lymphoblastic leukemia predicts relative glucocorticoid resistance that is overcome with MEK or Akt inhibition. *PLoS One*. 2019;14:e0220026.